



FPGA IMPLEMENTATION OF DISCRETE WAVELET TRANSFORM BASED SATELLITE IMAGE RESOLUTION ENHANCEMENT

M.Abinaya

AEC,Kumbakonam

abinayamaha@gmail.com

ABSTRACT

Satellite images are being used in many fields of research. One of the major issues of these types of images is their resolution. In this paper, we propose a new satellite image resolution enhancement technique based on the interpolation of the high-frequency subbands obtained by discrete wavelet transform(DWT) and the input image. The proposed resolution enhancement technique uses DWT to decompose the input image into different subbands. Then, the high-frequency subband images and the input low-resolution image have been interpolated, followed by combining all these images to generate a new resolution-enhanced image by using inverse DWT. In order to achieve a sharper image,an intermediate stage for estimating the high-frequency subbandshas been proposed. The proposed technique has been tested on satellite benchmark images. The quantitative (peak signal-to-noise ratio and root mean square error) and visual results show the superiority of the proposed technique over the conventional and state-of-art image resolution enhancement techniques.

Index Terms—Discrete wavelet transform (DWT), interpolation,satellite image resolution enhancement, wavelet zero padding (WZP).

1. INTRODUCTION

RESOLUTION of an image has been always an important issue in many image- and video-processing applications,such as video resolution enhancement [1], feature extraction [2], and satellite image resolution enhancement [3].Interpolation in image processing is a method to increase the number of pixels in a digital image. Interpolation has been widely used in many image processing applications, such as facial reconstruction [4], multiple description coding [5], and image resolution enhancement [6]–[8]. The interpolation-based image resolution enhancement has been used for a long time and many interpolation techniques have been developed to increase the quality of this task. There are three well-known interpolation techniques, namely, nearest neighbor, bilinear, and bicubic. Bicubic interpolation is more sophisticated than the other two techniques and produces smoother edges.Wavelets are also playing a significant role in many imageprocessing

applications. The 2-D wavelet decomposition of an image is performed by applying the 1-D discrete wavelet transform (DWT) along the rows of the image first, and then Manuscript received August 20, 2009; revised February 28, 2010 and August 12, 2010; accepted December 5, 2010. Date of publication January 27,2011; date of current version May 20, 2011. H. Demirel is with the Department of Electrical and Electronic Engineering, Eastern Mediterranean University, Gazima ğusa, Kuzey Kıbrıs Türk Cumhuriyeti, Mersin 10, Turkey (e-mail: hasan.demirel@emu.edu.tr).G. Anbarjafari is with the Department of Information Systems Engineering,Cyprus International

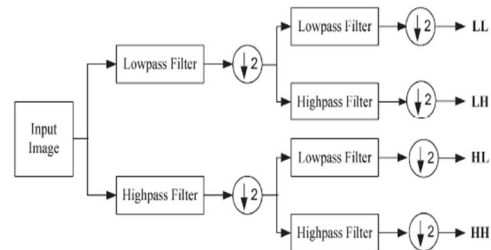
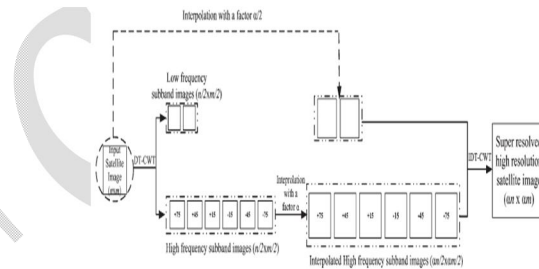
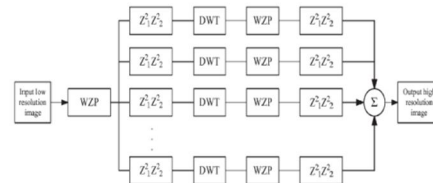




Figure. 1. LL, LH, HL, and HH subbands of a satellite image obtained by using DWT.

the results are decomposed along the columns. This operation results in four decomposed subband images referred to low-low (LL), low-high (LH), high-low (HL), and high-high (HH). The frequency components of those subbands cover the full frequency spectrum of the original image. Theoretically, a filter bank shown in Fig. 1 should operate on the image in order to generate different subband frequency images. Fig. 2 improve the sharpness of the reconstructed images [9]. Their estimation was carried out by investigating the evolution of wavelet transform extrema among the same type of subbands. Edges identified by an edge detection algorithm in lower frequency subbands were used to prepare a model for estimating edges in higher frequency subbands and only the coefficients with significant values were estimated as the evolution of the wavelet coefficients. In many researches, hidden Markov has been also implemented in order to estimate the coefficients [16]. In this paper, we propose resolution enhancement technique using interpolated DWT high-frequency subband images and the input low-resolution image. Inverse DWT (IDWT) has been applied to combine all these images to generate the final resolution-enhanced image. In order to achieve a sharper image, we propose to use an intermediate stage for estimating the high frequency subbands by utilizing the difference image obtained by subtracting the input image and its interpolated LL subband. The proposed technique has been compared with standard interpolation techniques, wavelet zero padding (WZP), where the unknown coefficients in high-frequency subbands are replaced with zeros, and state-of-art techniques, such as WZP and cyclespinning (CS) [17], and previously introduced

shows different subbands of a satellite image where the top left image is the LL subband, and the bottom right image is the HH subband. Image resolution enhancement using wavelets is a relatively new subject and recently many new algorithms have been proposed [9]–[15]. Carey *et al.* have attempted to estimate the unknown details of wavelet coefficients in an effort to



complex wavelet transform (CWT)-based image resolution enhancement [3]. It is necessary to recall that in this paper the resolution enhancement is used as a process that enlarges the given input in the way that the output is sharper. The performance of the proposed technique over performs all available state-of-art methods for image resolution enhancement. The visual and quantitative results are given in the results and discussions section. In all steps of the proposed satellite image resolution enhancement technique, Daubechies (db.9/7) wavelet transform as mother wavelet function and bicubic interpolation as interpolation technique have been used. The paper is organized as follows. Section II gives an overview on the state-of-art image resolution enhancement techniques used for comparison purposes. Section III introduces the proposed wavelet based resolution enhancement technique. Section IV discusses the qualitative and quantitative results of the proposed method with the conventional and state-of-art resolution enhancement techniques. Conclusions are given in the final section.

2. WAVELET-BASED IMAGE RESOLUTION ENHANCEMENT

There are several methods which have been used for satellite image resolution enhancement. In this

paper, we have used two state-of-art techniques for comparison purposes. The first one is WZP and CS [17], and the second one is the previously introduced CWT-based image resolution enhancement [3].

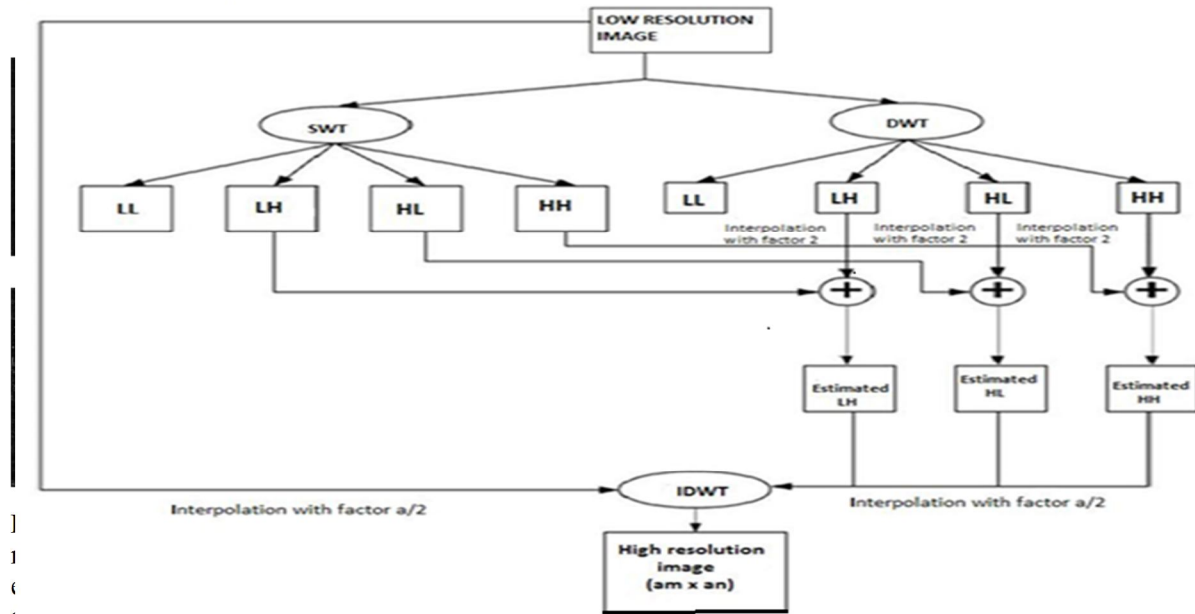
A. CS Based Image Resolution Enhancement

This method adopts the CS methodology in the waveletdomain [15]. The algorithm consists of two main steps as follows:

- 1) An initial approximation to the unknown high resolution image is generated using wavelet domain zero padding(WZP).
- 2) The cycle-spinning methodology is adopted to operate the following tasks:

- a) A number of low resolution images are generated from the obtained estimated high resolution image in part (1) by spatial shifting, wavelet transforming, and discarding the high frequency subbands.
- b) The WZP processing is applied to all those low resolution images yielding N high resolution images.
- c) These intermediated high resolution images are realignedand averaged to give the final high resolution reconstructed image.

Fig. 3 shows the block diagram of the WZP- and CS-based image super resolution.



enhancement technique.

B. CWT-Based Image Resolution Enhancement

In this technique, dual-tree CWT (DT-CWT) is used to decompose an input image into different

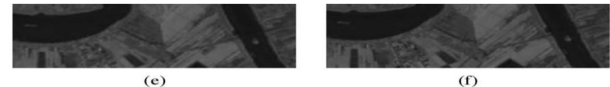


Fig. 8. (a), (b) Low-resolution image obtained from downsampling of the high-resolution image through DWT, (c) high-resolution image obtained by using bicubic interpolation with enlargement factor of four, (d) enhanced image obtained by WZP and CS technique, (e) and proposed method with the same enlargement factor. (f) The original high-resolution image.

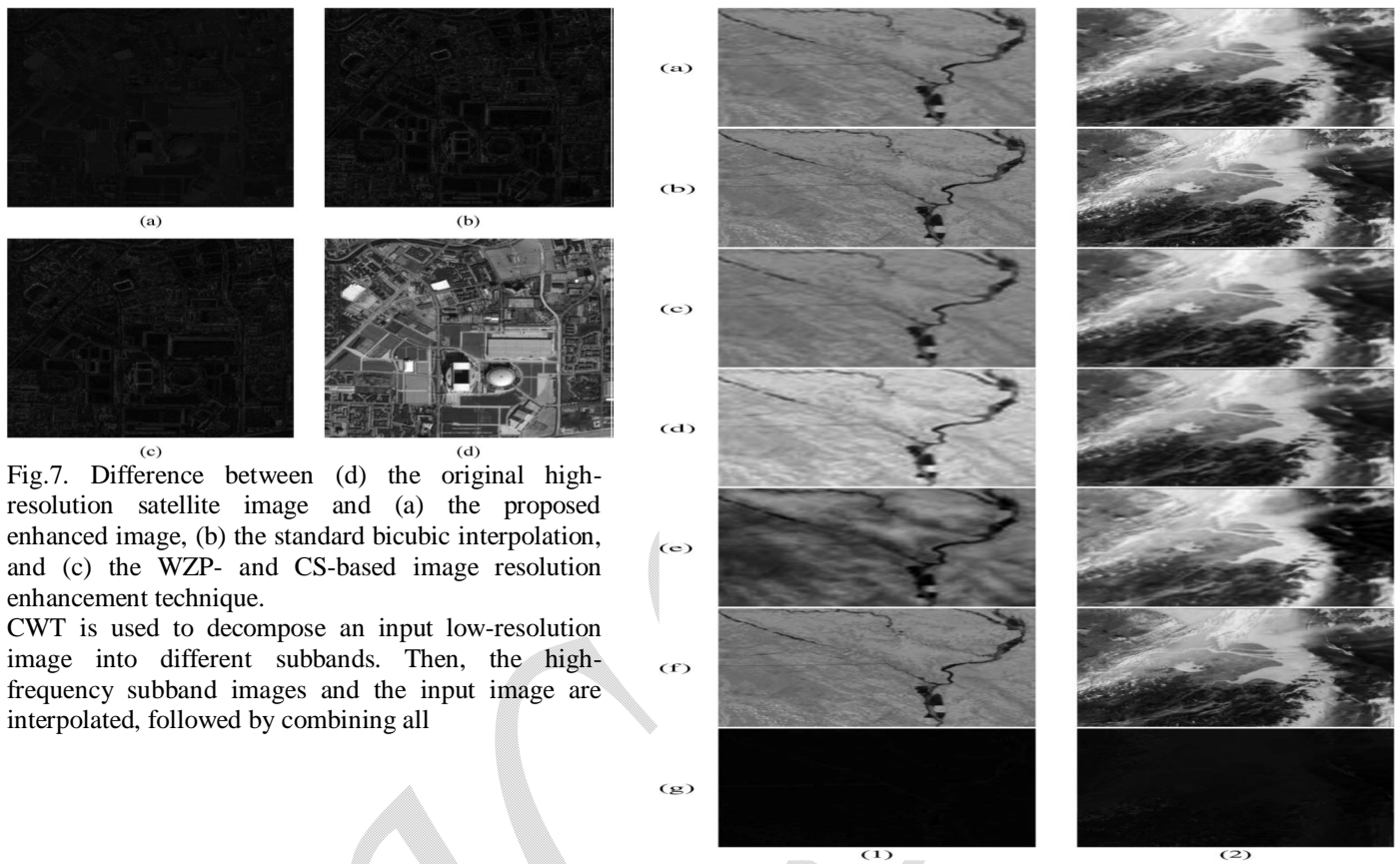


Fig.7. Difference between (d) the original high-resolution satellite image and (a) the proposed enhanced image, (b) the standard bicubic interpolation, and (c) the WZP- and CS-based image resolution enhancement technique.

CWT is used to decompose an input low-resolution image into different subbands. Then, the high-frequency subband images and the input image are interpolated, followed by combining all

these images to generate a new high-resolution image by using inverse DT-CWT. The resolution enhancement is achieved by using directional selectivity provided by the CWT, where the high-frequency subbands in six different directions contribute to the sharpness of the high-frequency details, such as edges. Details of this technique are shown in Fig. 4, where the enlargement factor through the resolution enhancement is α .

3. DWT-BASED RESOLUTION ENHANCEMENT

As it was mentioned before, resolution is an important feature in satellite imaging, which makes the resolution enhancement of such images to be of vital importance as increasing the resolution of these images will directly affect the performance of the system using these images as input. The main loss of an image after being resolution enhanced by applying interpolation is on its high-frequency components, which is due to the smoothing caused by interpolation. Hence, in order to increase the quality of the enhanced image, preserving the edges is essential. In this paper, DWT [19] has been employed in order to preserve the high-frequency components of the image. DWT separates the image into different subband images, namely, LL, LH, HL,

and HH. High-frequency subbands contains the high-frequency component of the image. The interpolation can be applied to these four subband images. In the wavelet domain, the low-resolution image is obtained by low-pass filtering of the high-resolution image as in [14], [17], and [19]. The low resolution image (LL subband), without quantization (i.e., with double-precision pixel values) is used as the input for the proposed resolution enhancement process. In other words, low-frequency subband images are the low resolution of the original image. Therefore, instead of using low-frequency subband images, which contains less information than the original input image, we are using this input image through the interpolation process. Hence, the input low-resolution image is interpolated with the half of the interpolation factor, $\alpha/2$, used to interpolate the high-frequency subbands, as shown in Fig. 5. In order to preserve more edge information, i.e., obtaining a sharper enhanced image, we have proposed an intermediate stage in high-frequency subband interpolation process. As shown in Fig. 5, the low-resolution input satellite image and the interpolated LL image with factor 2 are highly correlated. The difference between the LL subband image and the low-resolution input image are in their high-frequency components. Hence, this

difference image can be used in the intermediate process to correct the estimated high-frequency components. This estimation is performed by interpolating the high-frequency subbands by factor 2 and then including the difference image (which is high-frequency components on low-resolution input image)

into the estimated high-frequency images, followed by another interpolation with factor $\alpha/2$ in order to reach the required size for IDWT process. The intermediate process of adding the difference image, containing high-frequency components, generates significantly sharper and clearer final image. This sharpness is boosted by the fact that, the interpolation of isolated high-frequency components in HH, HL, and LH will preserve more high-frequency components than interpolating the low-resolution image directly.

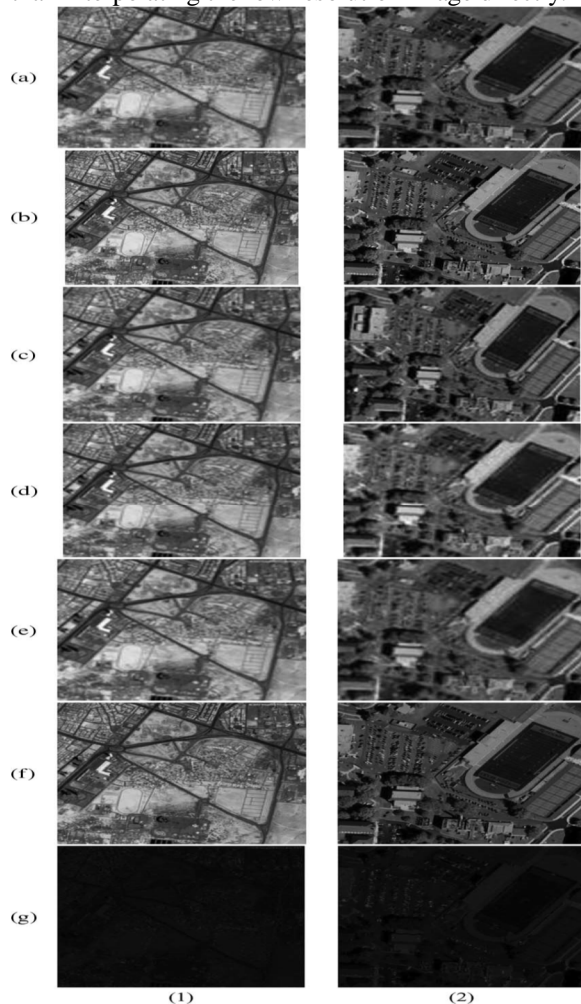


Fig. 10. (a) Low-resolution image obtained from downsampling of the high-resolution satellite image through 2 cascaded DWT, (b) original high-resolution satellite image, (c) bicubic interpolation-based resolution enhancement, (d) WZP, (e) WZP and CS technique, (f) the proposed image resolution enhancement technique, and (g) the difference between the original high-resolution satellite image and the image enhanced by the proposed technique with enlargement from 128×128 to 512×512 .

Figs. 6 and 7(a)–(c) show the difference between the high-resolution images with the enhanced image by using the proposed resolution enhancement technique, the difference obtained by using bicubic interpolation directly, and the difference image with WZP- and CS-based image resolution enhancement technique, respectively. Figs. 6 and 7(a) shows that more high-frequency components have been preserved in the proposed technique.

4. RESULTS AND DISCUSSIONS

The proposed technique has been tested on several different satellite images. In order to show the superiority of the proposed method over the conventional and state-of-art techniques from visual point of view Figs. 8–10 are included. In those figures with low-resolution satellite images, the enhanced images by using bicubic interpolation, enhanced images by using WZP and CS-based image resolution enhancement, and also the enhanced images obtained by the proposed technique are shown. It is clear that the resultant image, enhanced by using the proposed technique, is sharper than the other techniques.

FPGA Implementation of Discrete Wavelet Transform Based Satellite Image Resolution Enhancement

TABLE I
PSNR (DECIBELS) RESULTS FOR RESOLUTION ENHANCEMENT FROM 128 × 128 TO 512 × 512 PROPOSED TECHNIQUE COMPARED WITH CONVENTIONAL AND SOME STATE-OF-ART T

Method\Image	PSNR (dB)					
	Fig. 6	Fig. 7	Fig. 8	Fig. 9-1	Fig. 9-2	Fig. 10-1
Bilinear	19.07	21.02	25.78	28.94	23.67	20.91
Bicubic	20.16	22.87	26.29	29.54	24.05	21.30
WZP (Db. 9/7)	19.26	22.35	26.67	28.14	22.91	21.76
WZP and CS SR [15]	21.09	24.67	28.78	30.13	23.89	23.56
Demirel and Anbarjafari [3]	24.08	28.01	31.11	31.54	27.08	24.73
The proposed Method	24.97	29.33	32.67	33.49	30.22	26.03

TABLE II
RMSE RESULTS FOR RESOLUTION ENHANCEMENT FROM 128 × 128 TO 512 × 512 (α = 4) F TECHNIQUE COMPARED WITH CONVENTIONAL AND SOME STATE-OF-ART TECHN

Method\Image	RMSE					
	Fig. 6	Fig. 7	Fig. 8	Fig. 9-1	Fig. 9-2	Fig. 10-1
Bilinear	5.33	4.76	3.62	3.02	4.09	4.79
Bicubic	5.00	4.28	3.52	2.92	4.00	4.69
WZP (Db. 9/7)	5.27	4.41	3.44	3.16	4.27	4.56
WZP and CS SR [15]	4.74	3.86	3.05	2.82	4.04	4.11
Demirel and Anbarjafari [3]	3.99	3.18	2.66	2.60	3.36	3.85
The proposed Method	3.79	2.95	2.44	2.32	2.80	3.57

TABLE III
ENTROPY RESULTS FOR RESOLUTION ENHANCEMENT FROM 128 × 128 TO 512 × 512 (α = 4) FOR THE PROPOSED TECHNIQUE COMPARED WI PREVIOUSLY INTRODUCED RESOLUTION ENHANCEMENT TECHNIQUE [3], AS WELL AS LOW-RESOLUTION AND HIGH-RESOLUTION ORIGINAL IM.

Method\Image	Entropy			
	Fig. 9-1	Fig. 9-2	Fig. 10-1	Fig. 10-2
Low resolution satellite image (8-bit unsigned)	2.975	4.745	2.727	3.586
Low resolution satellite image (double precision)	5.8327	7.822	7.434	7.333
Original high resolution satellite image	5.968	7.872	7.578	7.484
Demirel and Anbarjafari [3]	5.936	7.758	7.423	7.189
The proposed Method	5.937	7.758	7.424	7.190

TABLE V
MSE RESULTS FOR RESOLUTION ENHANCEMENT FROM 128 × 128 TO 512 × 512 (α = 4) USING THE PROPOSED TECHNIQUE FOR THE QUANTIZED INPUT IMAGES (8-BIT UNSIGNED INTEGER), COMPARED WITH CONVENTIONAL AND SOME STATE-OF-ART TECHNIQUES

Method\Image	PSNR (dB)						
	Fig. 6	Fig. 7	Fig. 8	Fig. 9-1	Fig. 9-2	Fig. 10-1	Fig. 10-2
Bicubic	666.93	1230.50	237.73	278.02	968.46	1099.21	1177.82
WZP (Db. 9/7)	1210.82	1014.10	642.81	407.46	431.60	1202.49	993.30
WZP and CS SR [15]	507.08	847.38	253.56	100.71	370.75	798.14	314.83
Demirel and Anbarjafari [3]	1004.80	248.93	238.28	49.67	159.62	711.35	425.68
The proposed Method	408.39	236.09	226.51	35.90	82.43	381.14	67.16

Fig. 8 shows that a satellite image in (e) enhanced by using the proposed technique is clearly sharper than the low-resolution input image in (a) and (b), as well as the interpolated image in (c) and enhanced image by WZP and CS technique in (d). Figs. 9 and 10 show the effectiveness of the proposed method over the standard bicubic interpolation, WZP, and the state-of-art WZP- and CS-based image resolution enhancement techniques. Different benchmark images with different features are used for comparison.

Not only visual comparison but also quantitative comparisons are confirming the superiority of the proposed method. Peak signal-to-noise ratio (PSNR) and root mean square error (RMSE) have been implemented in order to obtain some quantitative results for comparison. PSNR can be obtained by using the following formula [20]:

$$PSNR = 10 \log_{10} \left(\frac{R^2}{MSE} \right) \quad (1)$$

TABLE VI
RMSE RESULTS FOR RESOLUTION ENHANCEMENT FROM 128 × 128 TO 512 × 512 (α = 4) USING THE PROPOSED TECHNIQUE FOR THE QUANTIZED INPUT IMAGES (8-BIT UNSIGNED INTEGER), COMPARED WITH CONVENTIONAL AND SOME STATE-OF-ART TECHNIQUES

Method\Image	PSNR (dB)					
	Fig. 6	Fig. 7	Fig. 8	Fig. 9-1	Fig. 9-2	Fig. 10-1
Bicubic	25.82	35.08	15.42	16.67	31.12	33.15
WZP (Db. 9/7)	34.80	31.84	25.35	20.19	20.77	34.68
WZP and CS SR [15]	22.52	29.11	15.92	10.04	19.25	28.25
Demirel and Anbarjafari [3]	31.70	15.78	15.44	7.05	12.63	26.67
The proposed Method	20.21	15.37	15.05	5.99	9.08	19.52

TABLE IV
PSNR (DECIBELS) RESULTS FOR RESOLUTION ENHANCEMENT FROM 128 × 128 TO 512 × 512 (α = 4) USING THE PROPOSED TECHNIQUE FOR THE QUANTIZED INPUT IMAGES (8-BIT UNSIGNED INTEGER), COMPARED WITH CONVENTIONAL AND SOME STATE-OF-ART TECHNIQUES

Method\Image	PSNR (dB)					
	Fig. 6	Fig. 7	Fig. 8	Fig. 9-1	Fig. 9-2	Fig. 10-1
Bicubic	19.89	17.23	24.37	23.69	18.27	17.72
WZP (Db. 9/7)	17.50	18.07	20.05	22.03	21.78	17.33
WZP and CS SR [15]	21.08	18.85	24.09	28.10	22.44	19.11
Demirel and Anbarjafari [3]	18.11	24.17	24.36	31.17	26.10	19.61
The proposed Method	22.02	24.40	24.58	32.58	28.97	22.32

where R is the maximum fluctuation in the input image (255 in here as the images are represented by 8 bit, i.e., 8-bit grayscale representation have been used radiometric resolution is 8 bit); and MSE is representing the MSE between the given input image I_{in} and the original image I_{org} which can be obtained by the following:

$$MSE = \frac{\sum_{i,j} (I_{in}(i,j) - I_{org}(i,j))^2}{M \times N} \quad (2)$$

where M and N are the size of the images. Clearly, RMSE is the square root of MSE, hence it can be calculated by the following:

$$RMSE = \sqrt{\frac{\sum_{i,j} (I_{in}(i,j) - I_{org}(i,j))^2}{M \times N}} \quad (3)$$

Table I is showing the comparison between the proposed method using Daubechies (db.9/7) wavelet transform with bicubic interpolation and some state-of-art resolution enhancement techniques, such as WZP, WZP and CS super-resolution technique [17], and also the formerly proposed resolution enhancement technique [3] by means of calculating PSNR. Table II is showing the comparison between the proposed method using Daubechies (db.9/7) wavelet transform with bicubic interpolation and aforementioned conventional and state-of-art techniques by means of RMSE. The results

in Table II are correlated with the results in Table I, which is expected due to the definition of the PSNR in (1). Overall, the results in Tables I and II show that the proposed method overperforms the aforementioned state-of-art and conventional techniques. In order to show the improvement obtained by the proposed satellite image resolution enhancement from information content point of view, the entropy of Figs. 9(1) and (2) and 10(1) and (2) have been calculated. Table III is showing these entropy values. As expected, highest level of information content is embedded in the original images. The main reason of having the relatively high information content level of the images generated by the proposed method is due to the fact that the unquantized input LL-subband images contain most of the information of the original high-resolution image. A possible unsigned 8-bit representation of the LL-subband image would introduce irreversible quantization loss of information which is given in the first row of Table III. As it was mentioned in the previous section, the low-resolution input images are obtained by downsampling the high-resolution images. This approach can be tolerated in some applications where there is no limitation in the number of bits for the representation of floating point numbers. However, in some applications, the downsampled images have to go through a quantization process where the fractions are removed to accommodate 8-bit unsigned integer representation. In order to show the effect of the quantization loss embedded in 8-bit unsigned integer representation, the proposed resolution enhancement technique has been applied to quantized images, and the results are reported in Tables IV–VI. The results are confirming the expectation of performance drop on the proposed algorithm due to the loss of information contained in the floating points. However, this drop is also encountered in other conventional and state-of-the-art techniques. The visual results corresponding to the quantized input image given in Fig. 10(2-a) are given in Fig. 11.

5. CONCLUSION

This paper has proposed a new resolution enhancement technique based on the interpolation of the high-frequency subband images obtained by DWT and the input image. The proposed technique has been tested on well-known benchmark images, where their PSNR and RMSE and visual results show the superiority of the proposed technique over the conventional and state-of-art image resolution enhancement techniques.

The PSNR improvement of the proposed technique is up to 7.19 dB compared with the standard bicubic

interpolation.

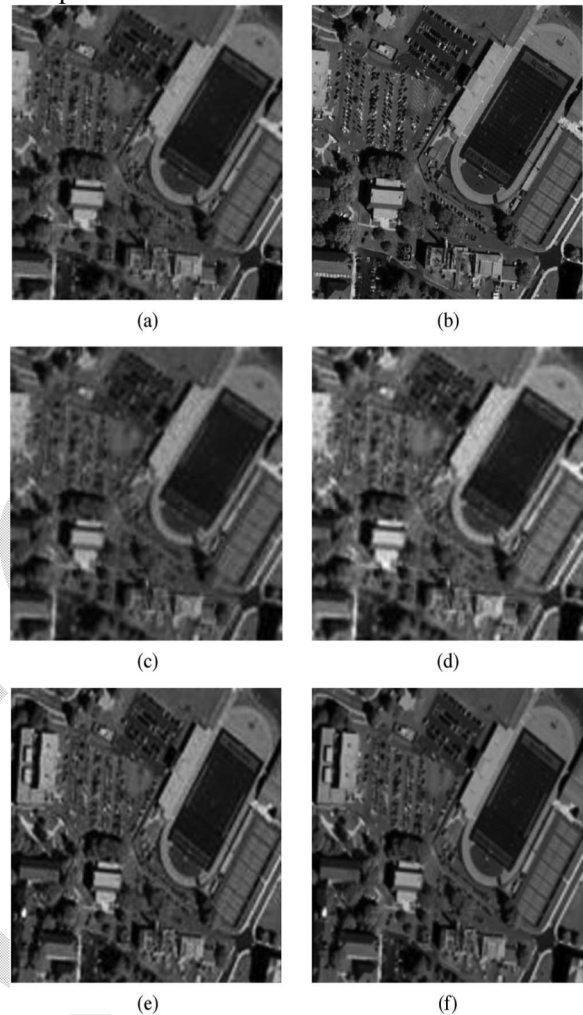


Fig. 11. (a) Quantized low-resolution image, (b) original high-resolution satellite image, (c) bicubic interpolation-based resolution enhancement, (d) WZP, (e) WZP and CS technique, (f) the proposed image resolution enhancement technique, with enlargement from 128×128 to 512×512 .

ACKNOWLEDGMENT

The authors would like to thank Dr. A. Temizel from Bilkent University for providing the output of the WZP- and CS-based resolution enhancement technique [14]. Moreover, the authors would like to acknowledge Prof. Dr. I. Selesnick from Polytechnic

University for providing the DWT codes in MATLAB. Furthermore, the authors would like to thank Google Earth and Satellite Imaging Corporation for providing satellite images for research purposes.

REFERENCES

- [1] H. Demirel, G. Anbarjafari, and S. Izadpanahi, "Improved motion-based localized super resolution technique using discrete wavelet transform for low resolution video enhancement," in *Proc. 17th EUSIPCO*, Edinburgh, U.K., Aug. 2009, pp. 1097–1101.
- [2] T. Celik, C. Direkoglu, H. Ozkaramanli, H. Demirel, and M. Uyguroglu, "Region-based super-resolution aided facial feature extraction from low resolution video sequences," in *Proc. IEEE ICASSP*, Philadelphia, PA, Mar. 2005, vol. II, pp. 789–792.
- [3] H. Demirel and G. Anbarjafari, "Satellite image resolution enhancement using complex wavelet transform," *IEEE Geosci. Remote Sens. Lett.*, vol. 7, no. 1, pp. 123–126, Jan. 2010.
- [4] L. Yi-bo, X. Hong, and Z. Sen-yue, "The wrinkle generation method for facial reconstruction based on extraction of partition wrinkle line features and fractal interpolation," in *Proc. 4th ICIG*, Aug. 22–24, 2007, pp. 933–937.
- [5] Y. Rener, J. Wei, and C. Ken, "Downsample-based multiple description coding and post-processing of decoding," in *Proc. 27th CCC*, Jul. 16–18, 2008, pp. 253–256.
- [6] C. B. Atkins, C. A. Bouman, and J. P. Allebach, "Optimal image scaling using pixel classification," in *Proc. ICIP*, Oct. 7–10, 2001, vol. 3, pp. 864–867.
- [7] Y. Piao, L. Shin, and H. W. Park, "Image resolution enhancement using inter-subband correlation in wavelet domain," in *Proc. IEEE ICIP*, 2007, vol. 1, pp. I-445–I-448.
- [8] G. Anbarjafari and H. Demirel, "Image super resolution based on interpolation of wavelet domain high frequency subbands and the spatial domain input image," *ETRI J.*, vol. 32, no. 3, pp. 390–394, Jun. 2010.
- [9] W. K. Carey, D. B. Chuang, and S. S. Hemami, "Regularity-preserving image interpolation," *IEEE Trans. Image Process.*, vol. 8, no. 9, pp. 1295–1297, Sep. 1999.
- [10] X. Li and M. T. Orchard, "New edge-directed interpolation," *IEEE Trans. Image Process.*, vol. 10, no. 10, pp. 1521–1527, Oct. 2001.
- [11] K. Kinebuchi, D. D. Muresan, and T.W. Parks, "Image interpolation using wavelet based hidden Markov trees," in *Proc. IEEE ICASSP*, 2001, vol. 3, pp. 7–11.
- [12] M. S. Crouse, R. D. Nowak, and R. G. Baraniuk, "Wavelet-based statistical signal processing using hidden Markov models," *IEEE Trans. Signal Process.*, vol. 46, no. 4, pp. 886–902, Apr. 1998.
- [13] S. Zhao, H. Han, and S. Peng, "Wavelet domain HMT-based image super resolution," in *Proc. IEEE ICIP*, Sep. 2003, vol. 2, pp. 933–936.
- [14] A. Temizel and T. Vlachos, "Image resolution upscaling in the wavelet domain using directional cycle spinning," *J. Electron. Imaging*, vol. 14, no. 4, p. 040501, 2005.
- [15] A. Gambardella and M. Migliaccio, "On the superresolution of microwave scanning radiometer measurements," *IEEE Geosci. Remote Sens. Lett.*, vol. 5, no. 4, pp. 796–800, Oct. 2008.
- [16] V. A. Tolpekin and A. Stein, "Quantification of the effects of land-cover class spectral separability on the accuracy of Markov-random-field-based superresolution mapping," *IEEE Trans. Geosci. Remote Sens.*, vol. 47, no. 9, pp. 3283–3297, Sep. 2009.
- [17] A. Temizel and T. Vlachos, "Wavelet domain image resolution enhancement using cycle-spinning," *Electron. Lett.*, vol. 41, no. 3, pp. 119–121, Feb. 3, 2005.
- [18] L. A. Ray and R. R. Adhami, "Dual tree discrete wavelet transform with application to image fusion," in *Proc. 38th Southeastern Symp. Syst. Theory*, Mar. 5–7, 2006, pp. 430–433.
- [19] A. Temizel, "Image resolution enhancement using wavelet domain hidden Markov tree and coefficient sign estimation," in *Proc. ICIP*, 2007, vol. 5, pp. V-381–V-384.
- [20] R. C. Gonzalez and R. E. Woods, *Digital Image Processing*. Englewood Cliffs, NJ: Prentice-Hall, 2007.